

Supplementary Materials: Heteroleptic [Cu(P[^]P)(N[^]N)][PF₆] Compounds with Isomeric Dibromo-1,10-Phenanthroline Ligands

Isaak Nohara, Aramis Keller, Nikolai Tarassenko, Alessandro Prescimone, Edwin C. Constable, and Catherine E. Housecroft *

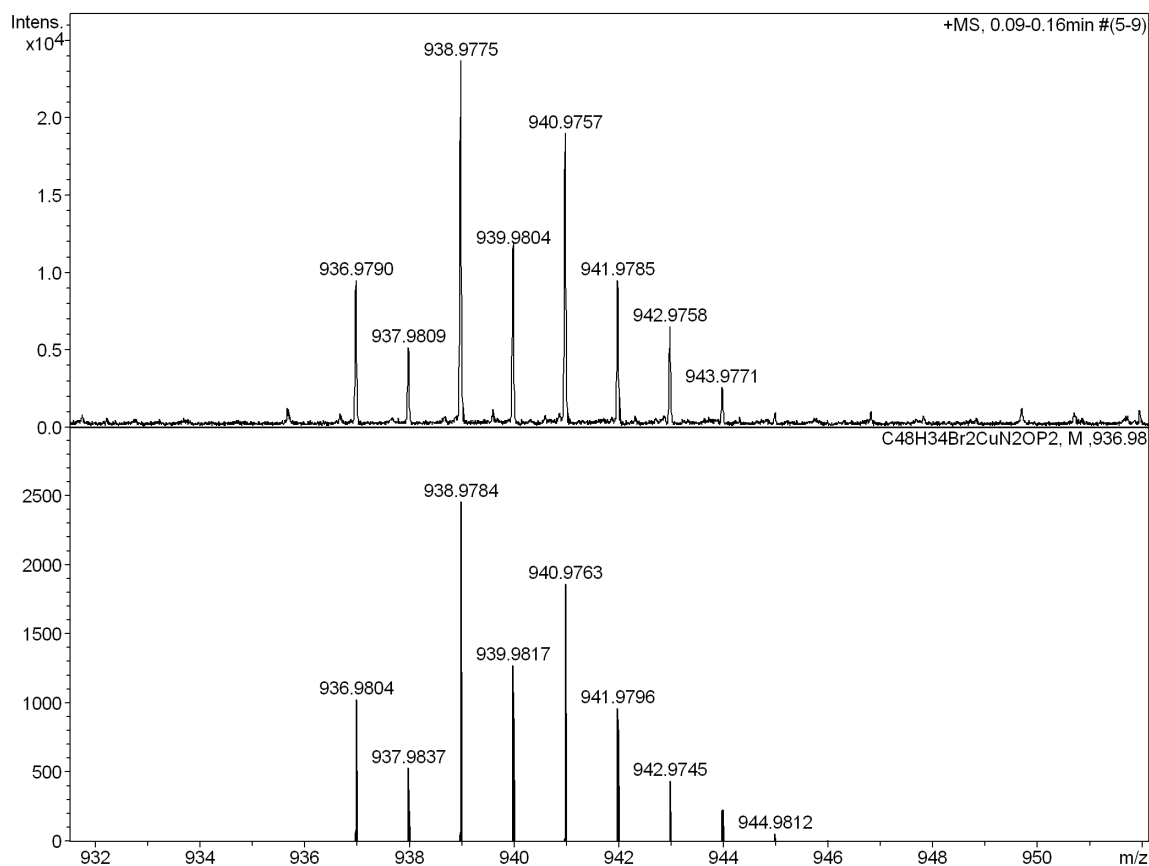
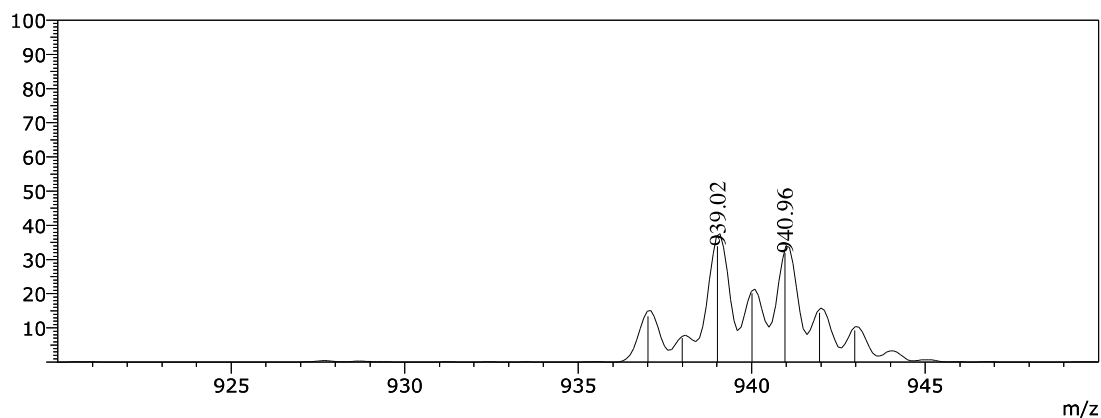


Fig. S1. The [M-PF₆]⁺ peak in the high-resolution electrospray mass spectrum of [Cu(POP)(2,9-Br₂phen)][PF₆]: top, observed and bottom, calculated.

Line#:1 R.Time:----(Scan#:----) MS Spectrum Positive Full Scan Zoomed View
 MassPeaks:20
 Spectrum Mode:Averaged 0.007-0.180(3-55) Base Peak:601.09(572243)
 BG Mode:Averaged 0.247-2.993(75-899) Segment 1 - Event 1



Line#:1 R.Time:----(Scan#:----) MS Spectrum Positive Full Scan Zoomed View
 MassPeaks:20
 Spectrum Mode:Averaged 0.007-0.180(3-55) Base Peak:601.09(572243)
 BG Mode:Averaged 0.247-2.993(75-899) Segment 1 - Event 1

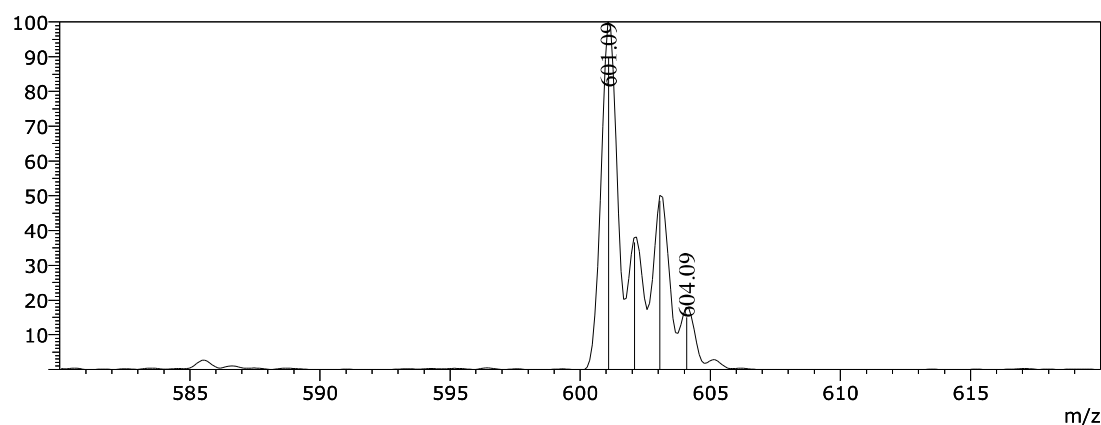


Fig. S2. Expansions of the peaks for the $[M-PF_6]^+$ and $[Cu(POP)]^+$ ions in the ESI mass spectrum of $[Cu(POP)(2,9-Br_2phen)][PF_6]$.

Line#:1 R.Time:0.067(Scan#:9) MS Spectrum Positive Full Scan Zoomed View
 MassPeaks:15
 Spectrum Mode:Single 0.067(9) Base Peak:701.47(222400)
 BG Mode:None Segment 1 - Event 1

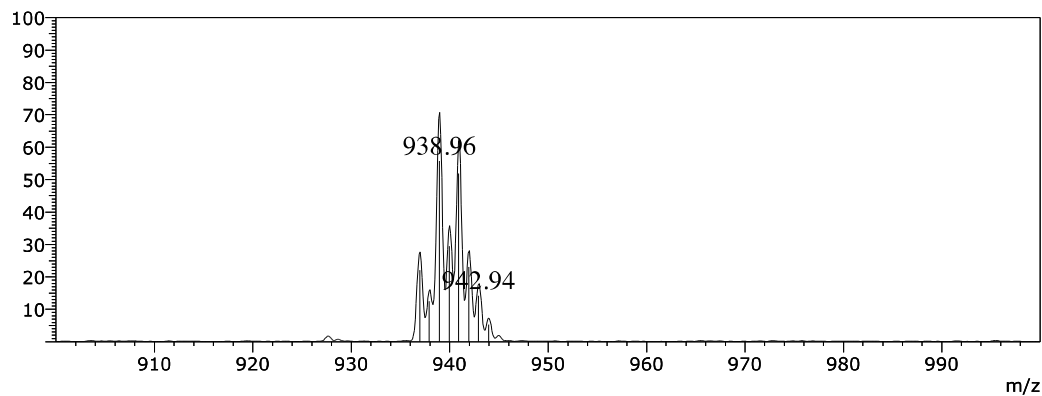


Fig. S3. Expansion of the peak for the $[M-PF_6]^+$ ion in the ESI mass spectrum of $[Cu(POP)(3,8-Br_2phen)][PF_6]$.

Line#:1 R.Time:0.050(Scan#:7) MS Spectrum Positive Full Scan Zoomed View
MassPeaks:23
Spectrum Mode:Single 0.050(7) Base Peak:701.48(1921266)
BG Mode:None Segment 1 - Event 1

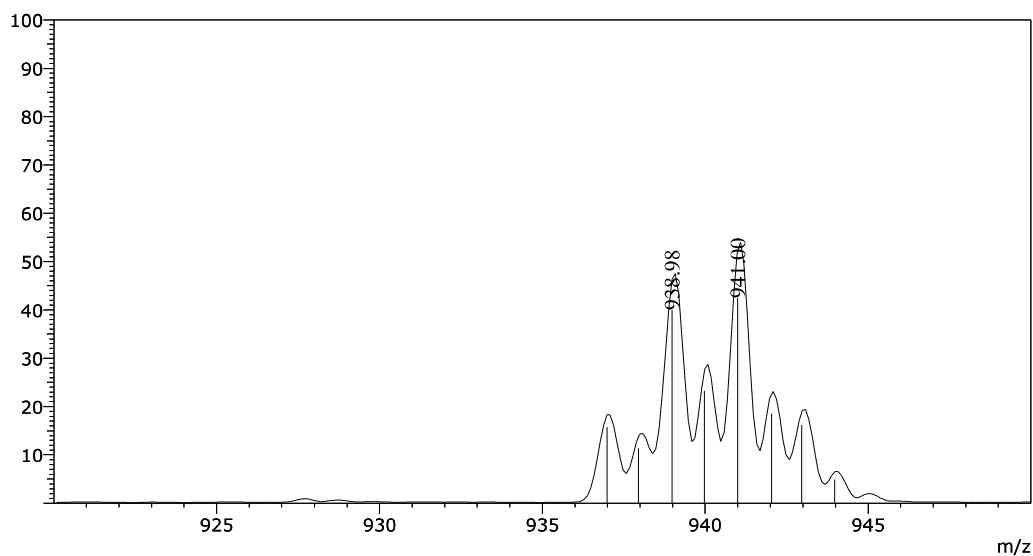
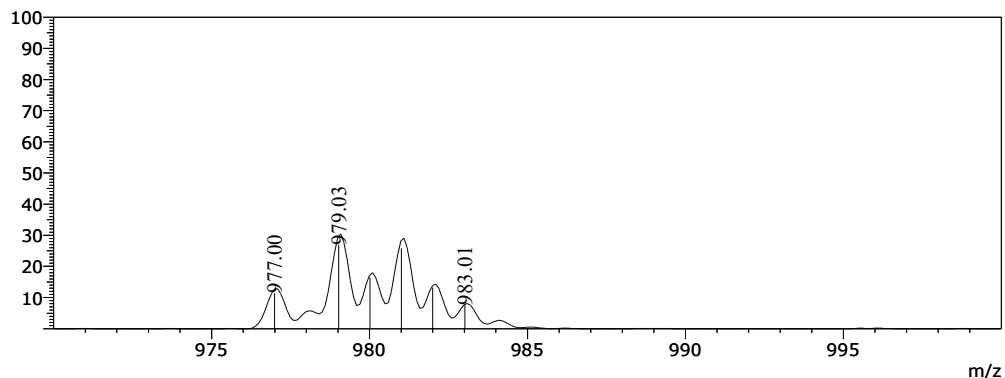


Fig. S4. Expansion of the peak for the $[M-PF_6]^+$ ion in the ESI mass spectrum of $[Cu(POP)(4,7-Br_2phen)][PF_6]$.

Line#:1 R.Time:----(Scan#:----) MS Spectrum Positive Full Scan Zoomed View
MassPeaks:20
Spectrum Mode:Averaged 0.013-0.147(5-45) Base Peak:475.29(465278)
BG Mode:Averaged 0.233-0.953(71-287) Segment 1 - Event 1



Line#:1 R.Time:----(Scan#:----) MS Spectrum Positive Full Scan Zoomed View
MassPeaks:20
Spectrum Mode:Averaged 0.013-0.147(5-45) Base Peak:475.29(465278)
BG Mode:Averaged 0.233-0.953(71-287) Segment 1 - Event 1

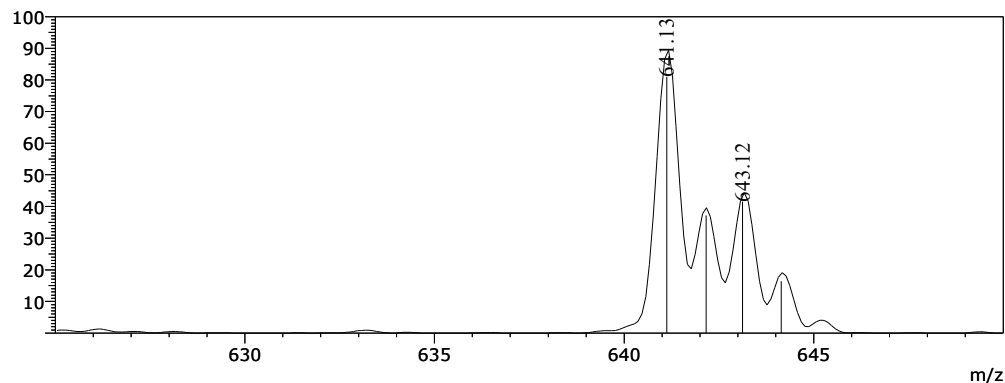


Fig. S5. Expansions of the peaks for the $[M-PF_6]^+$ and $[Cu(xantphos)]^+$ ions in the ESI mass spectrum of $[Cu(xantphos)(2,9-Br_2phen)][PF_6]$.

Line#:1 R.Time:0.067(Scan#:9) MS Spectrum Positive Full Scan Zoomed View
MassPeaks:31
Spectrum Mode:Single 0.067(9) Base Peak:528.49(1650476)
BG Mode:None Segment 1 - Event 1

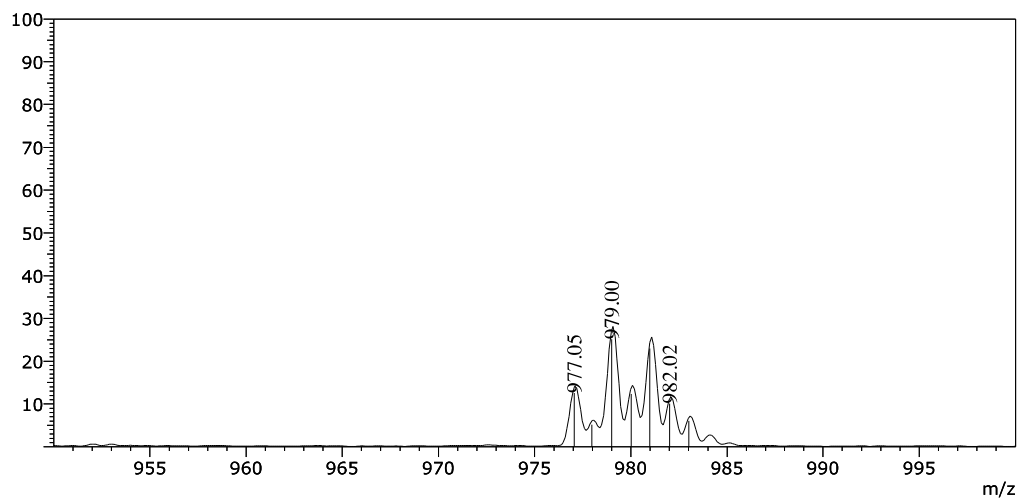


Fig. S6. Expansion of the peak for the $[M-PF_6]^+$ ion in the ESI mass spectrum of $[Cu(xantphos)(3,8-Br_2phen)][PF_6]$.

Line#:1 R.Time:-----(Scan#:----) MS Spectrum Positive Full Scan Zoomed View
MassPeaks:20
Spectrum Mode:Averaged 0.013-0.113(5-35) Base Peak:475.30(810959)
BG Mode:Averaged 0.507-1.387(153-417) Segment 1 - Event 1

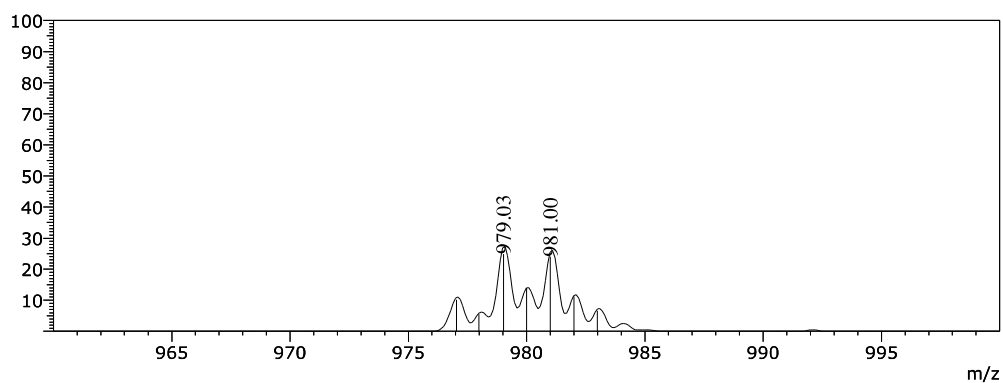


Fig. S7. Expansion of the peak for the $[M-PF_6]^+$ ion in the ESI mass spectrum of $[Cu(xantphos)(4,7-Br_2phen)][PF_6]$.

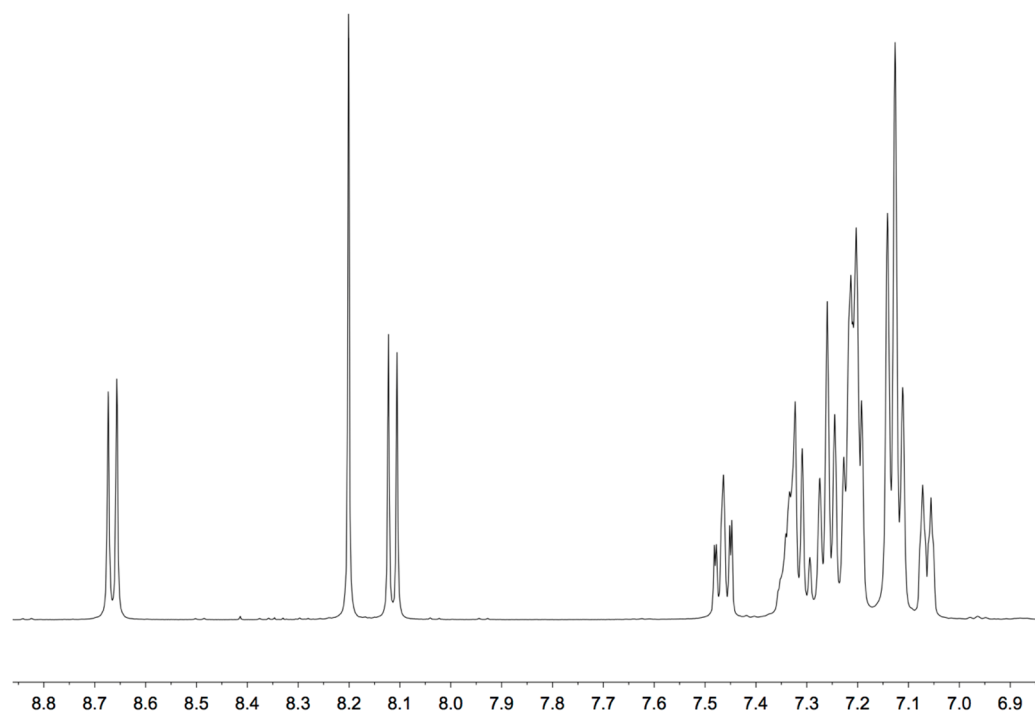


Fig. S8. Aromatic region of the ^1H NMR spectrum (500 MHz, acetone- d_6 , 298 K) of $[\text{Cu}(\text{POP})(2,9\text{-Br}_2\text{phen})][\text{PF}_6]$.

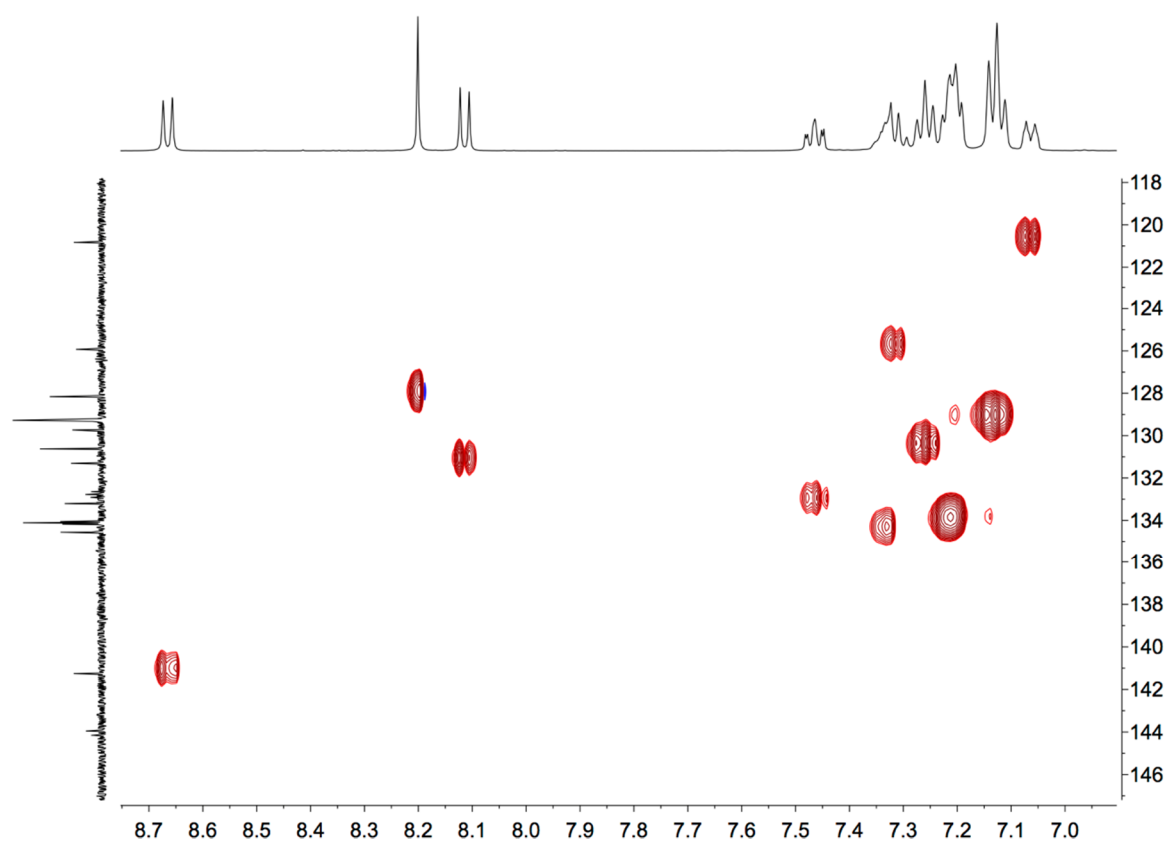


Fig. S9. HMQC spectrum (500 MHz ^1H , 126 MHz $^{13}\text{C}\{^1\text{H}\}$, acetone- d_6 , 298 K) of $[\text{Cu}(\text{POP})(2,9\text{-Br}_2\text{phen})][\text{PF}_6]$.

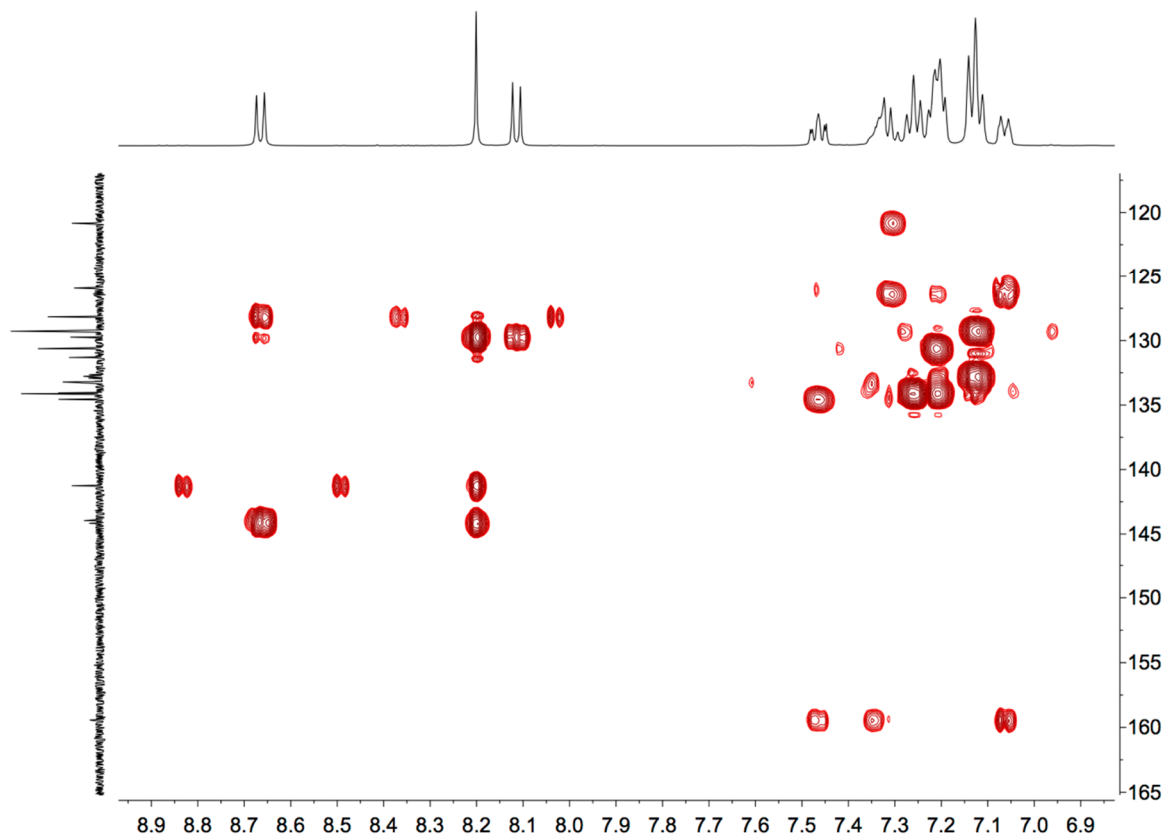


Fig. S10. HMBC spectrum (500 MHz ^1H , 126 MHz $^{13}\text{C}\{^1\text{H}\}$, acetone- d_6 , 298 K) of $[\text{Cu}(\text{POP})(2,9\text{-Br}_2\text{phen})][\text{PF}_6]$.

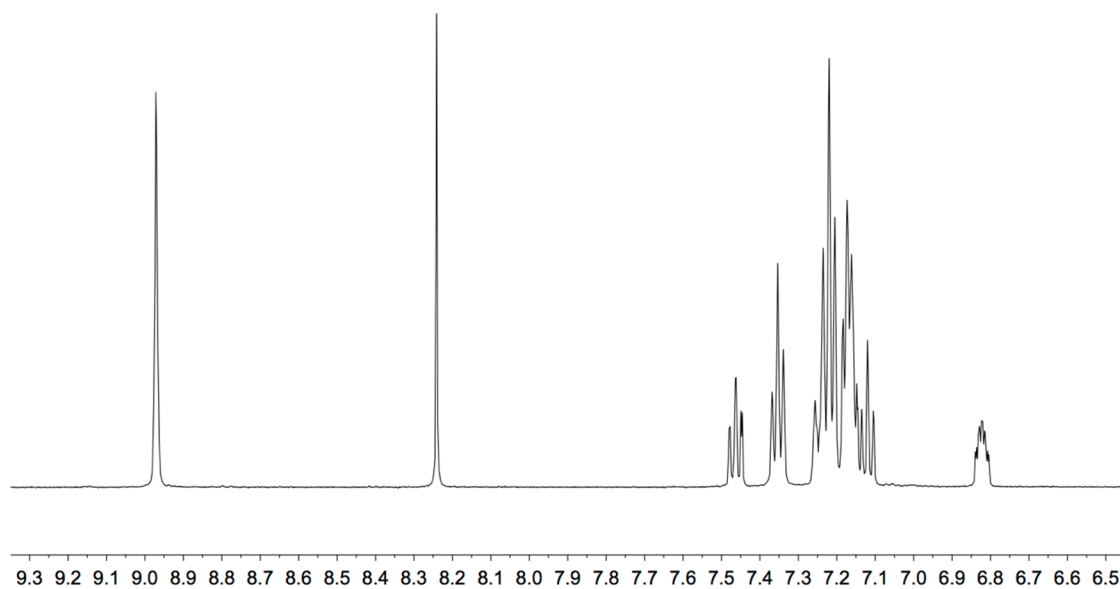


Fig. S11. Aromatic region of the ^1H NMR spectrum (500 MHz, acetone- d_6 , 298 K) of $[\text{Cu}(\text{POP})(3,8\text{-Br}_2\text{phen})][\text{PF}_6]$.

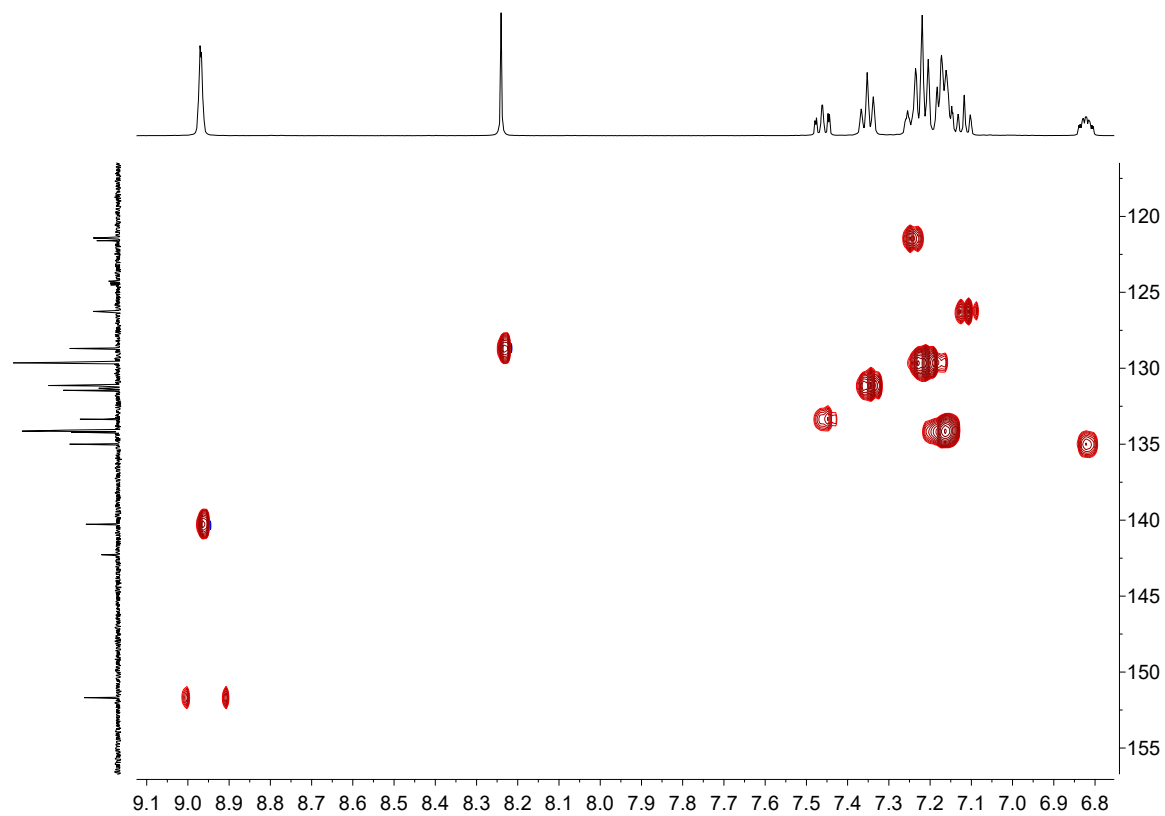


Fig. S12. HMPC spectrum (500 MHz ^1H , 126 MHz $^{13}\text{C}\{^1\text{H}\}$, acetone- d_6 , 298 K) of $[\text{Cu}(\text{POP})(3,8\text{-Br}_2\text{phen})][\text{PF}_6]$.

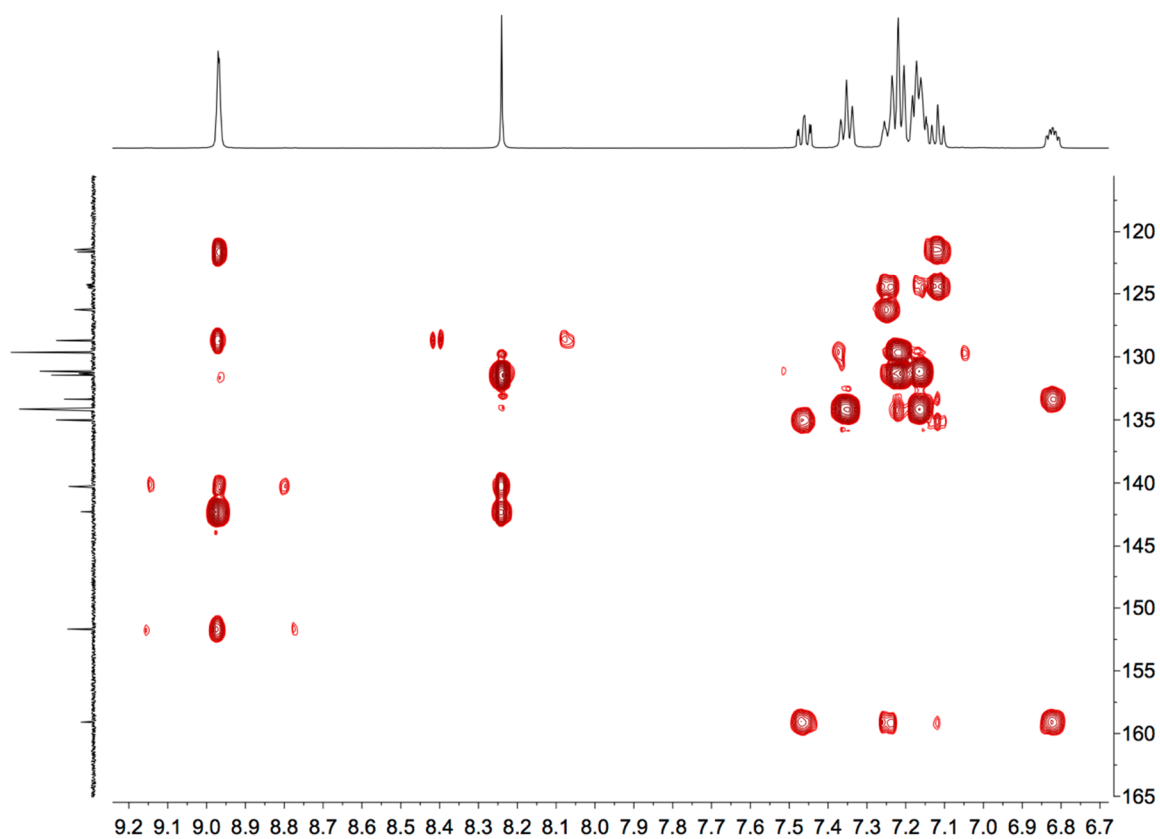


Fig. S13. HMBC spectrum (500 MHz ^1H , 126 MHz $^{13}\text{C}\{^1\text{H}\}$, acetone- d_6 , 298 K) of $[\text{Cu}(\text{POP})(3,8\text{-Br}_2\text{phen})][\text{PF}_6]$.

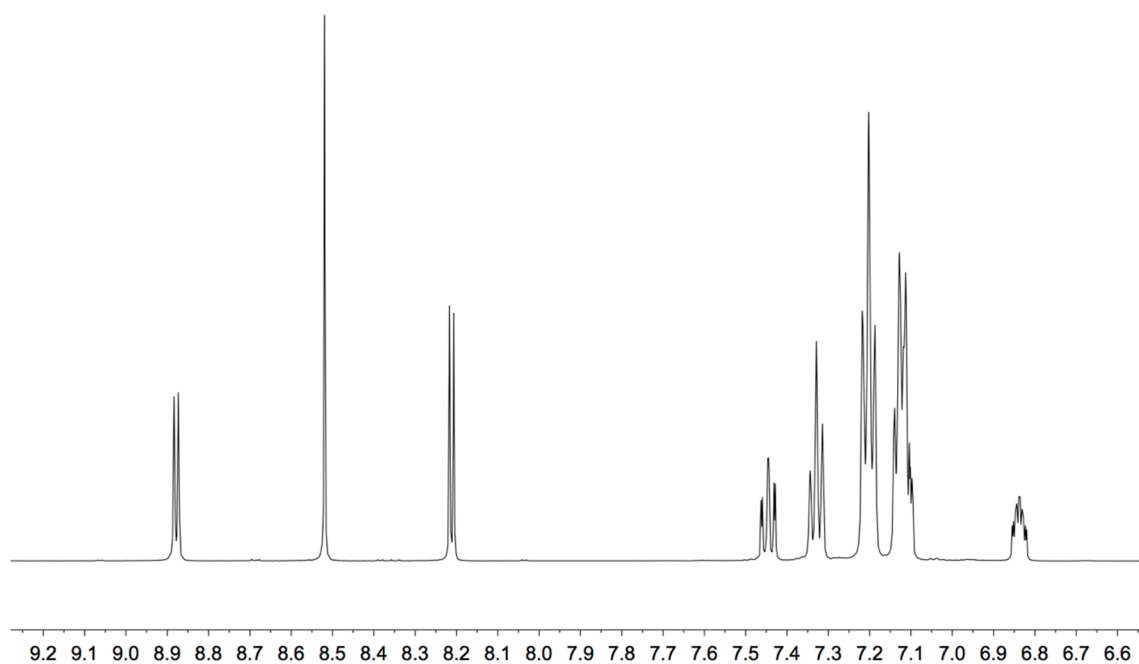


Fig. S14. Aromatic region of the ^1H NMR spectrum (500 MHz, acetone- d_6 , 298 K) of $[\text{Cu}(\text{POP})(4,7\text{-Br}_2\text{phen})][\text{PF}_6]$.

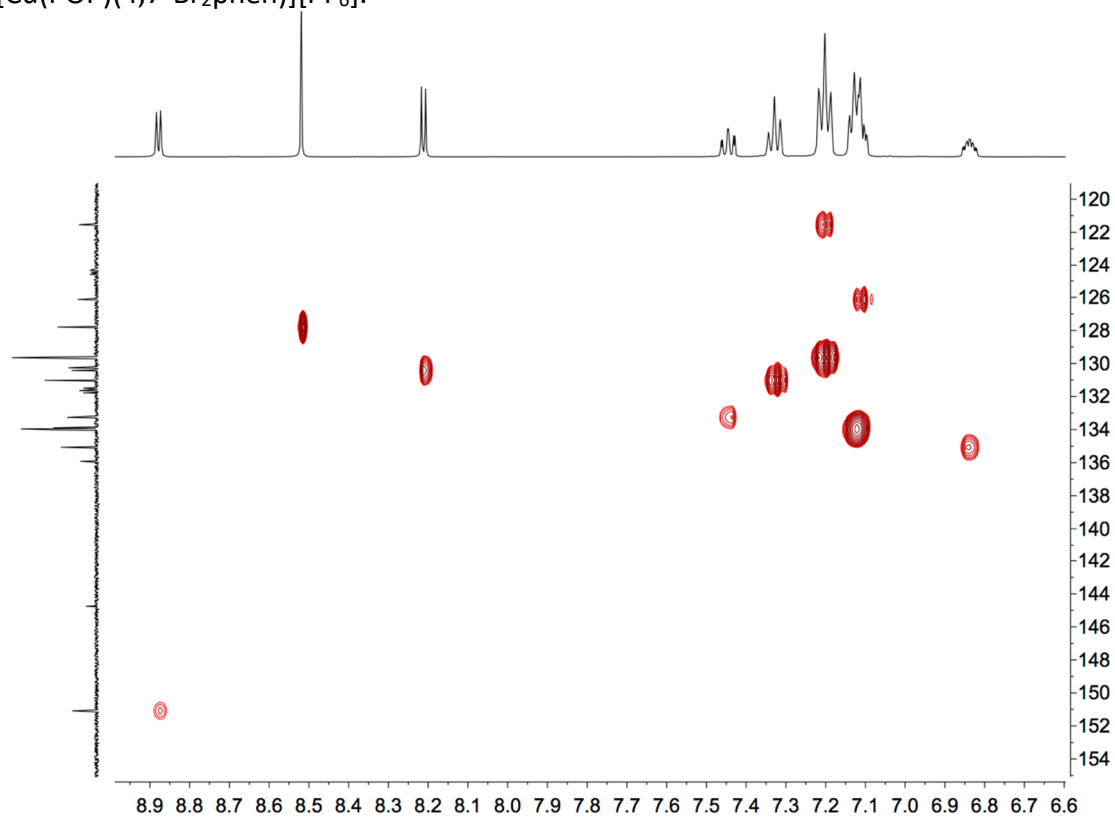


Fig. S15. HMQC spectrum (500 MHz ^1H , 126 MHz $^{13}\text{C}\{^1\text{H}\}$, acetone- d_6 , 298 K) of $[\text{Cu}(\text{POP})(4,7\text{-Br}_2\text{phen})][\text{PF}_6]$.

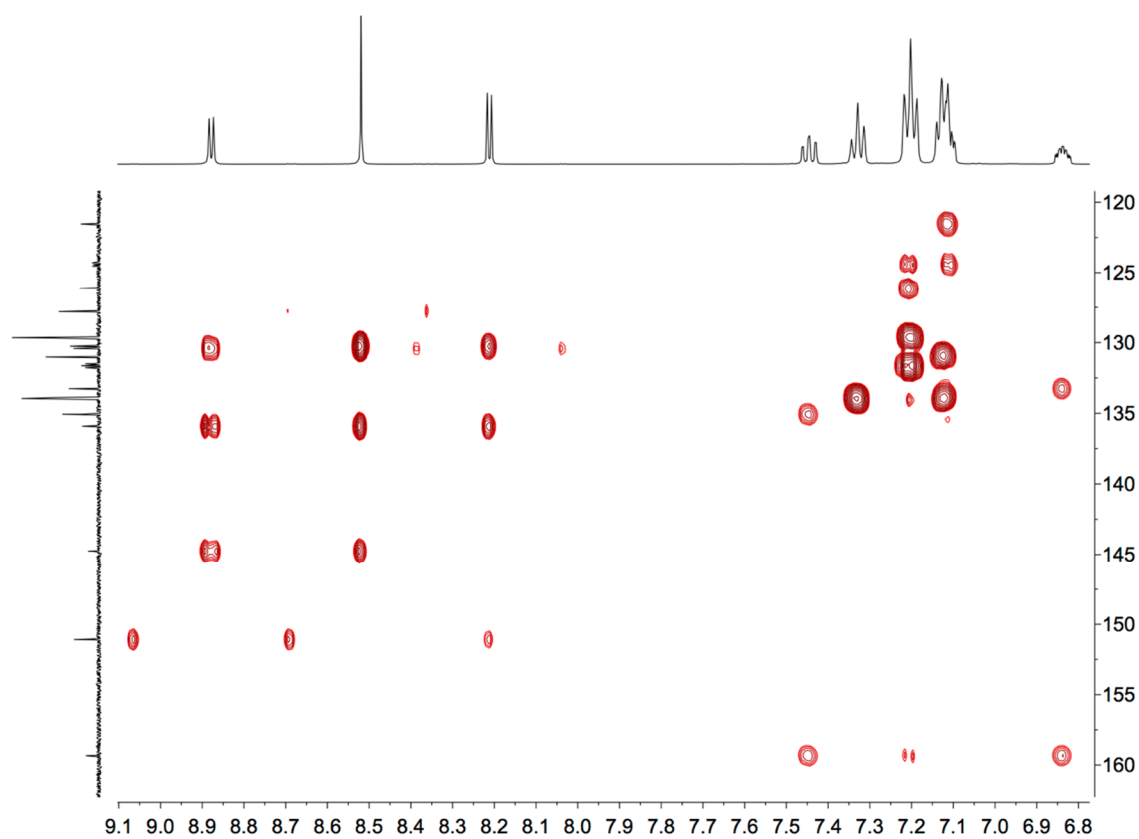


Fig. S16. HMBC spectrum (500 MHz ^1H , 126 MHz $^{13}\text{C}\{^1\text{H}\}$, acetone- d_6 , 298 K) of $[\text{Cu}(\text{POP})(4,7\text{-Br}_2\text{phen})][\text{PF}_6]$.

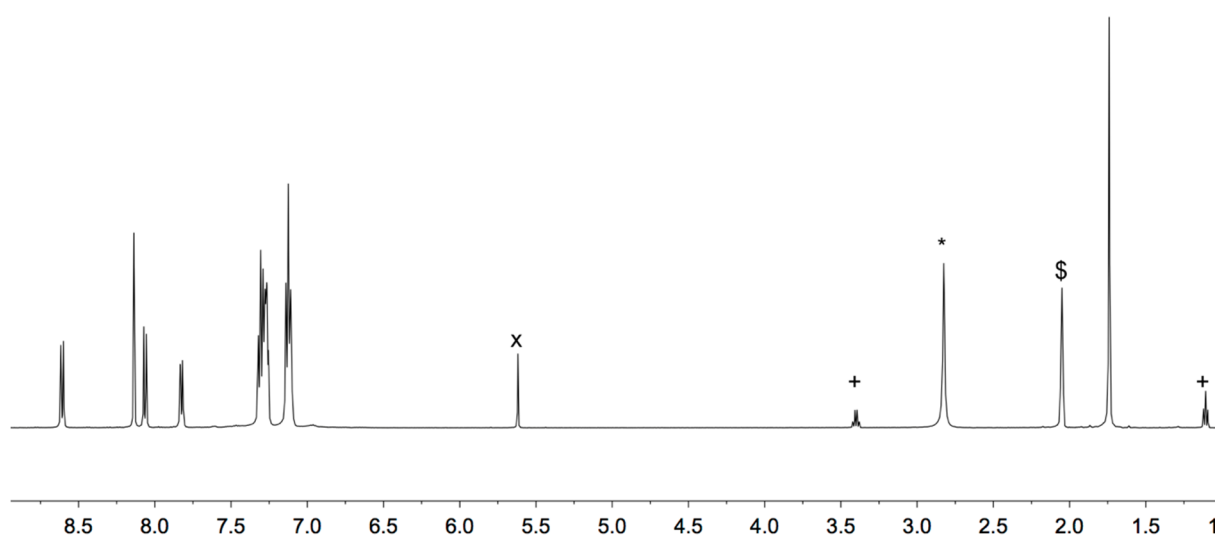


Fig. S17. ^1H NMR spectrum (500 MHz, acetone- d_6 , 298 K) of $[\text{Cu}(\text{xantphos})(2,9\text{-Br}_2\text{phen})][\text{PF}_6]$. \$ = acetone- d_5 ; * = H_2O ; + = Et_2O ; x = CH_2Cl_2 .

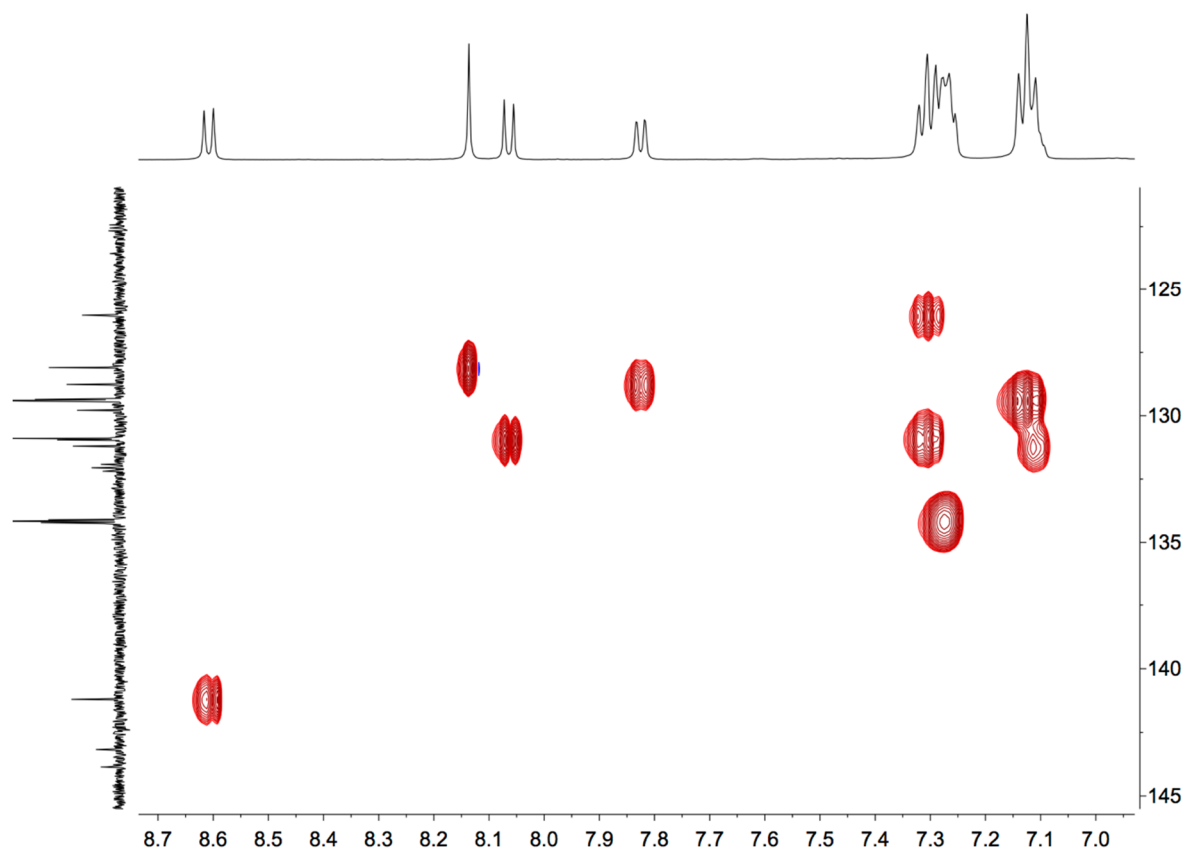


Fig. S18. HMQC spectrum (aromatic region, 500 MHz ¹H, 126 MHz ¹³C{¹H}, acetone-*d*₆, 298 K) of [Cu(xantphos)(2,9-Br₂phen)][PF₆].

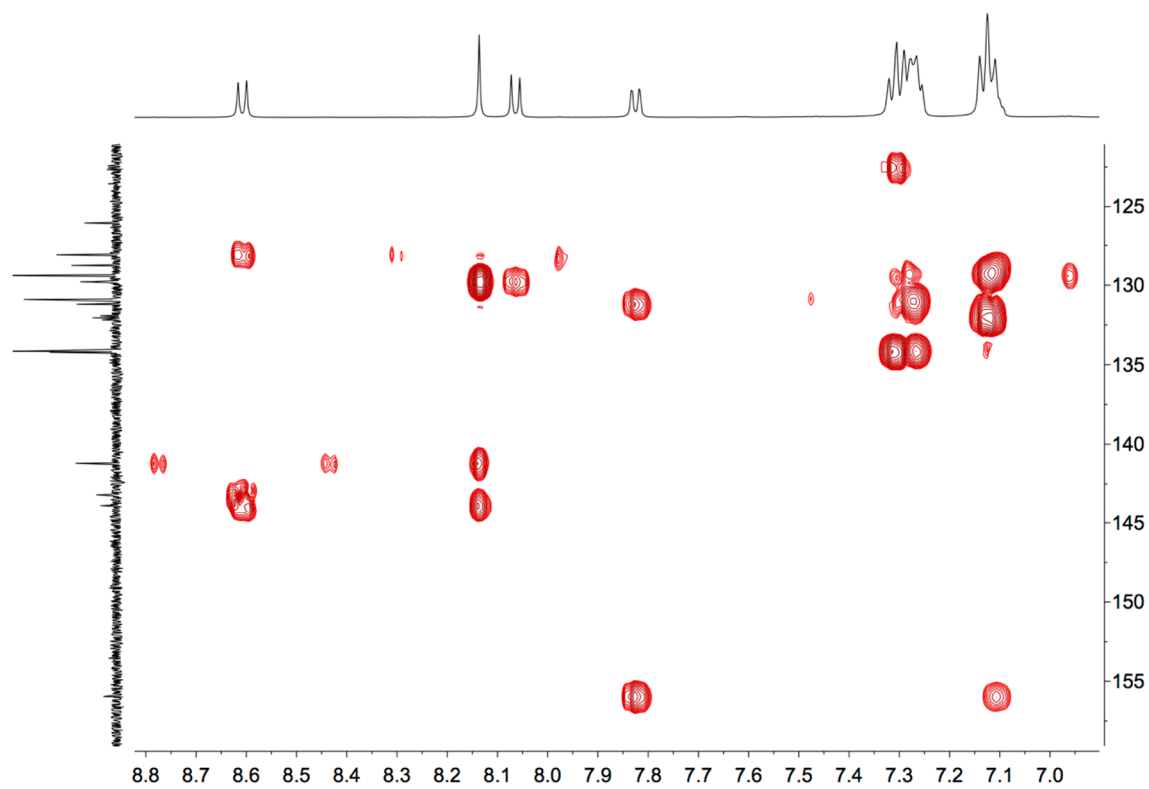


Fig. S19. HMBC spectrum (aromatic region, 500 MHz ^1H , 126 MHz $^{13}\text{C}\{^1\text{H}\}$, acetone- d_6 , 298 K) of $[\text{Cu}(\text{xantphos})(2,9\text{-Br}_2\text{phen})][\text{PF}_6]$.

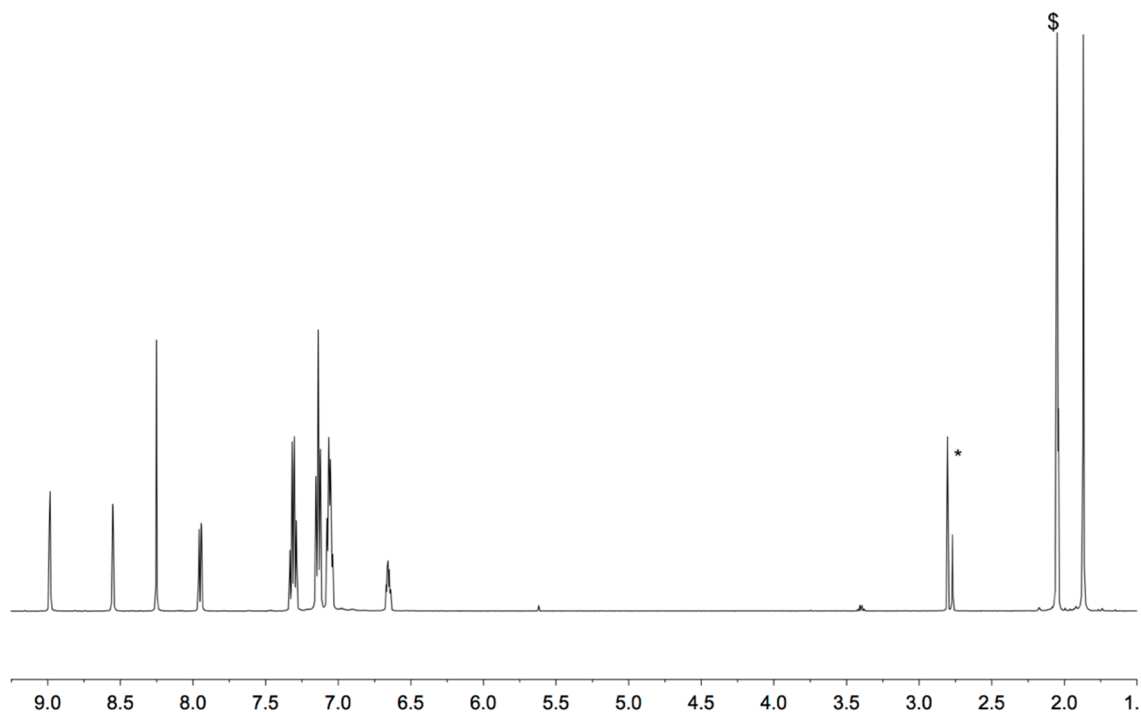


Fig. S20. ^1H NMR spectrum (500 MHz, acetone- d_6 , 298 K) of $[\text{Cu}(\text{xantphos})(3,8\text{-Br}_2\text{phen})][\text{PF}_6]$. \$ = acetone- d_5 ; * = H₂O and HOD.

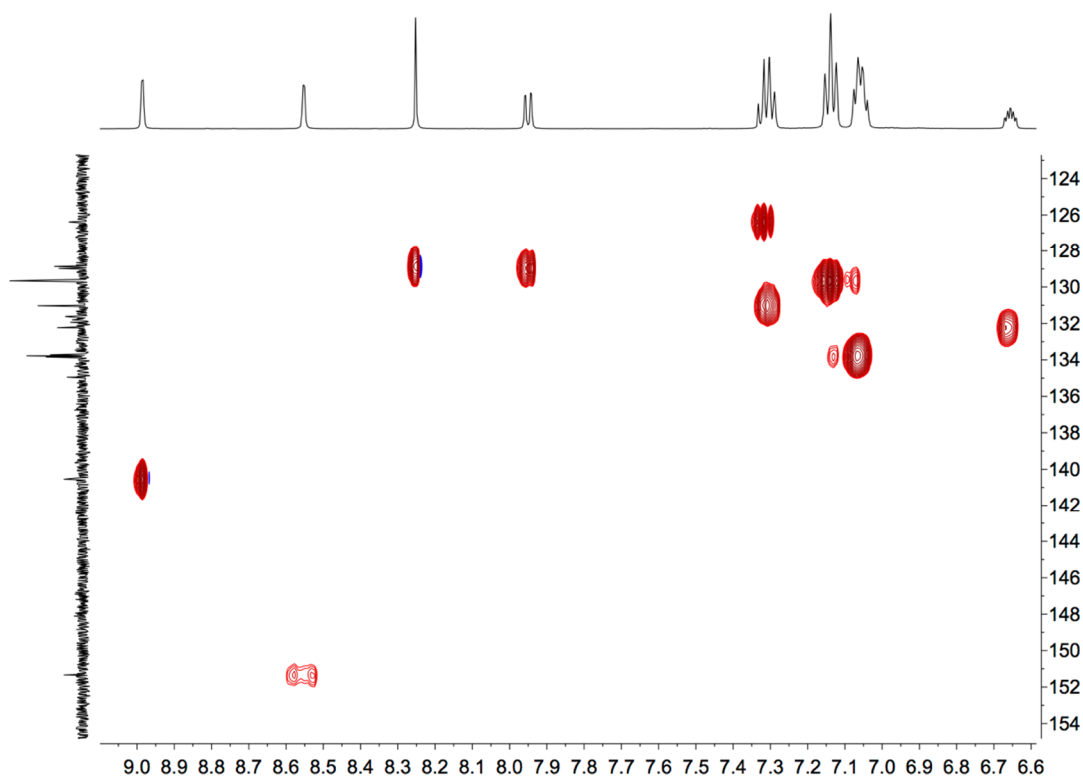


Fig. S21. HMQC spectrum (aromatic region, 500 MHz ^1H , 126 MHz $^{13}\text{C}\{^1\text{H}\}$, acetone- d_6 , 298 K) of $[\text{Cu}(\text{xantphos})(3,8\text{-Br}_2\text{phen})][\text{PF}_6]$.

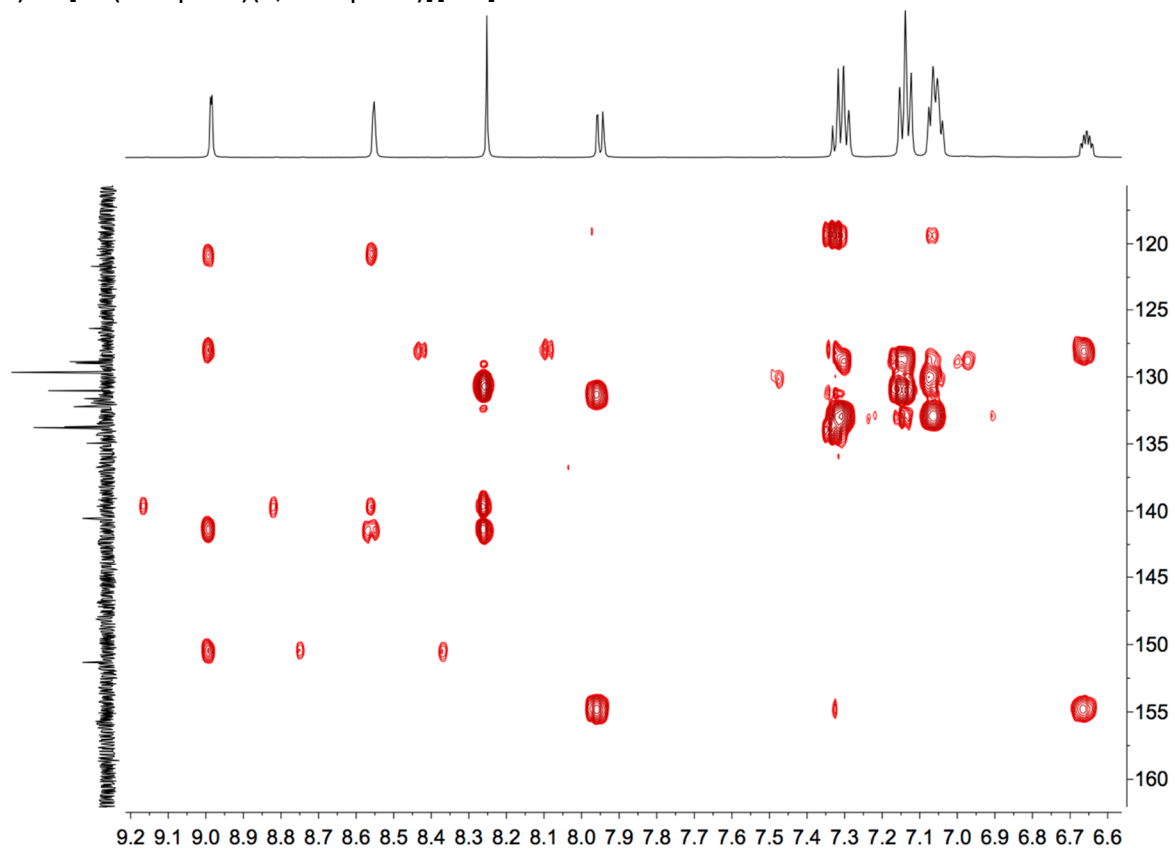


Fig. S22. HMBC spectrum (aromatic region, 500 MHz ^1H , 126 MHz $^{13}\text{C}\{^1\text{H}\}$, acetone- d_6 , 298 K) of $[\text{Cu}(\text{xantphos})(3,8\text{-Br}_2\text{phen})][\text{PF}_6]$.

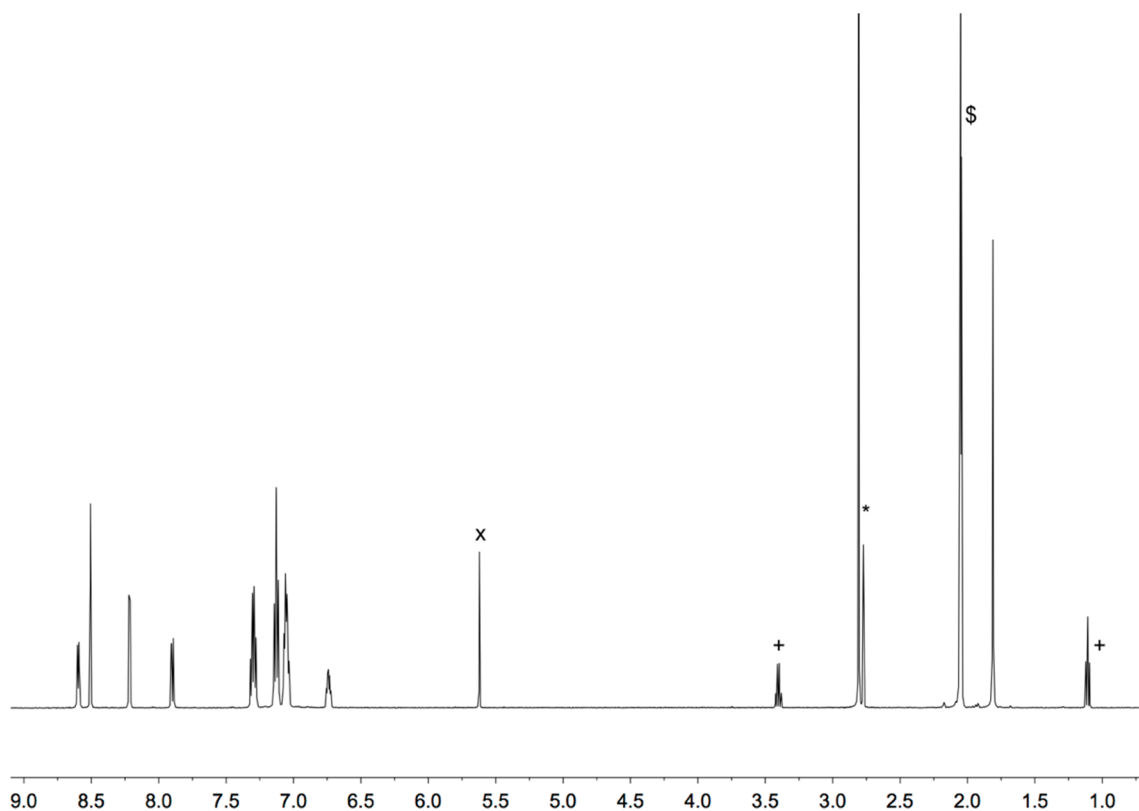


Fig. S23. ^1H NMR spectrum (500 MHz, acetone- d_6 , 298 K) of $[\text{Cu}(\text{xantphos})(4,7\text{-Br}_2\text{phen})][\text{PF}_6]$. $\$$ = acetone- d_5 ; * = H_2O and HOD ; x = CH_2Cl_2 ; + = Et_2O .

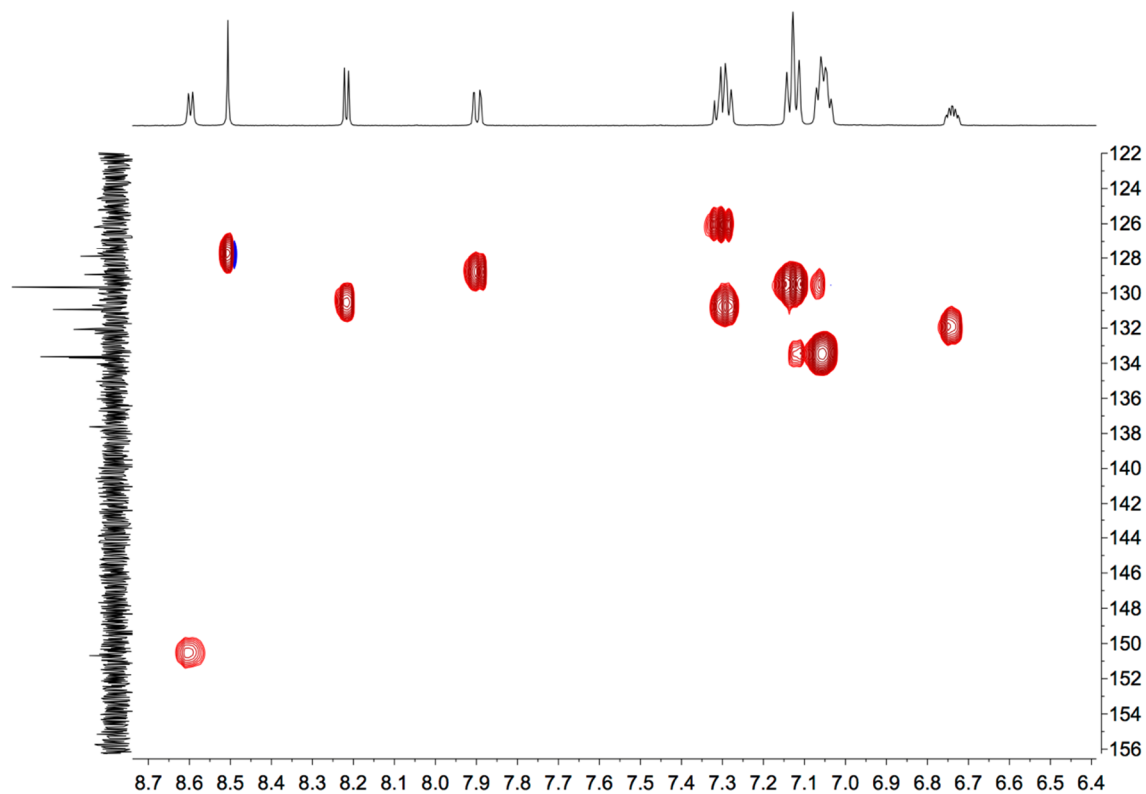


Fig. S24. HMQC spectrum (aromatic region, 500 MHz ^1H , 126 MHz $^{13}\text{C}\{^1\text{H}\}$, acetone- d_6 , 298 K) of $[\text{Cu}(\text{xantphos})(4,7\text{-Br}_2\text{phen})][\text{PF}_6]$.

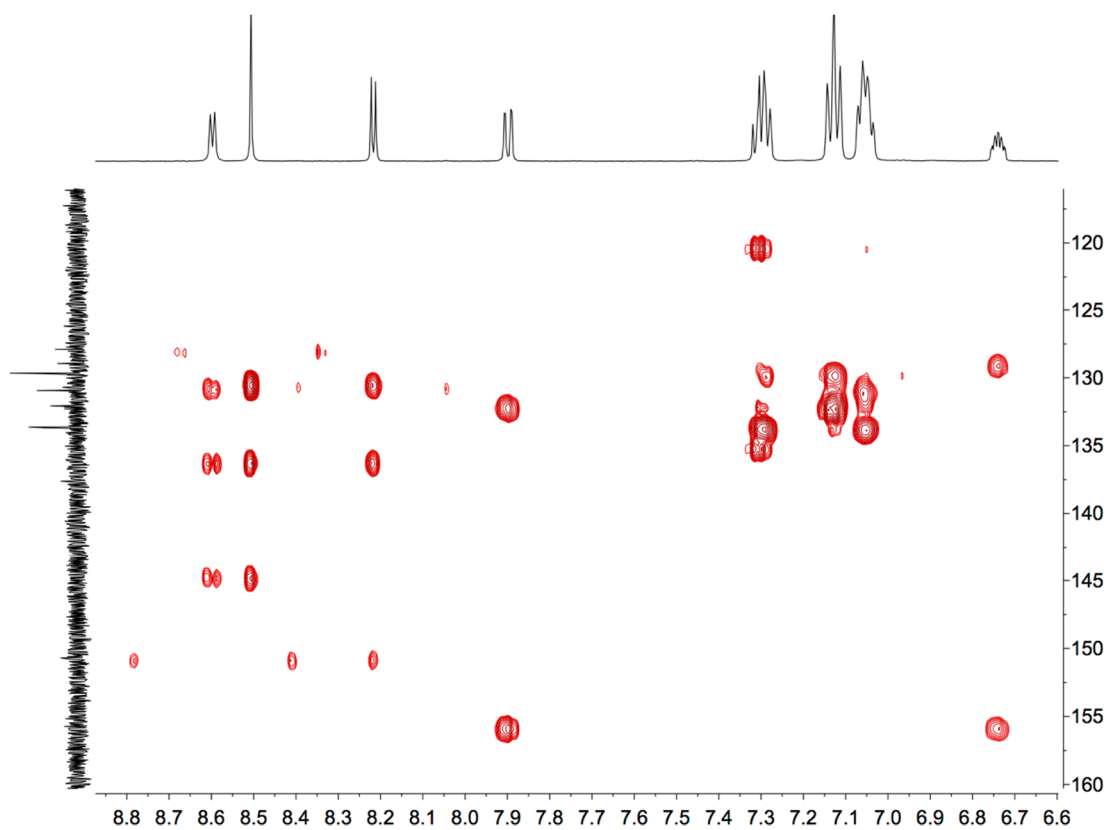
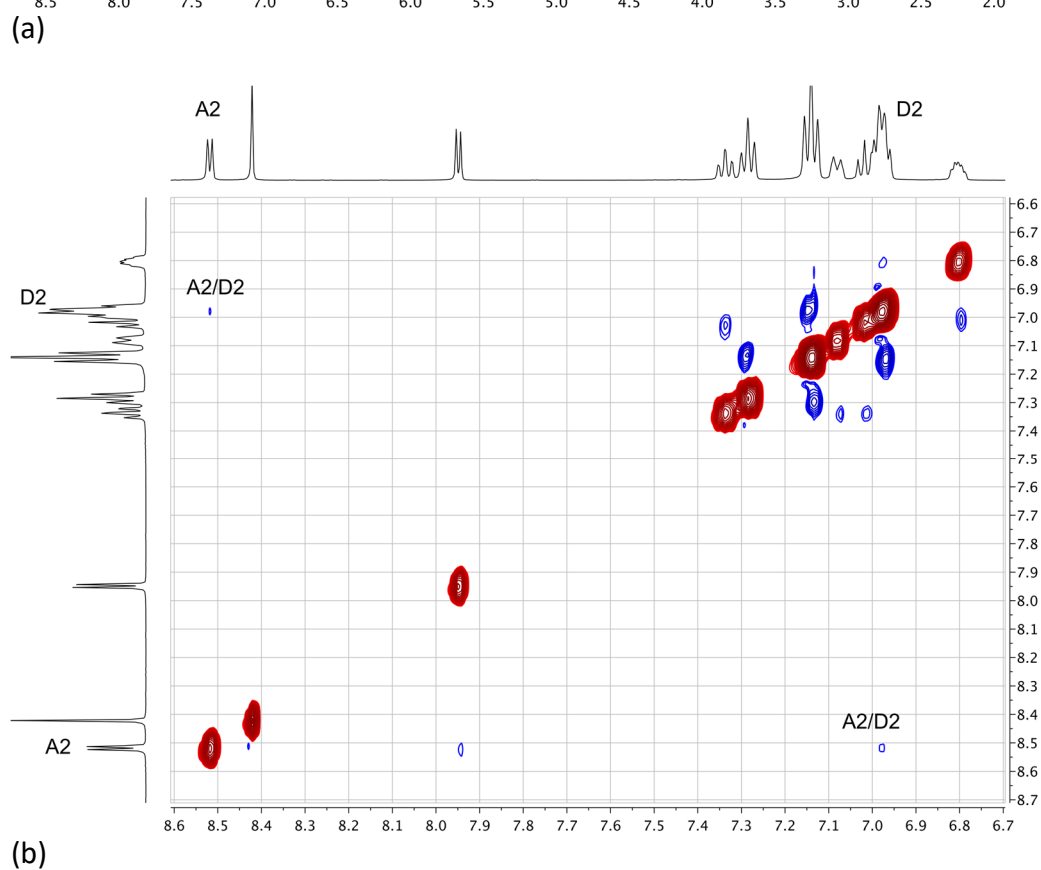
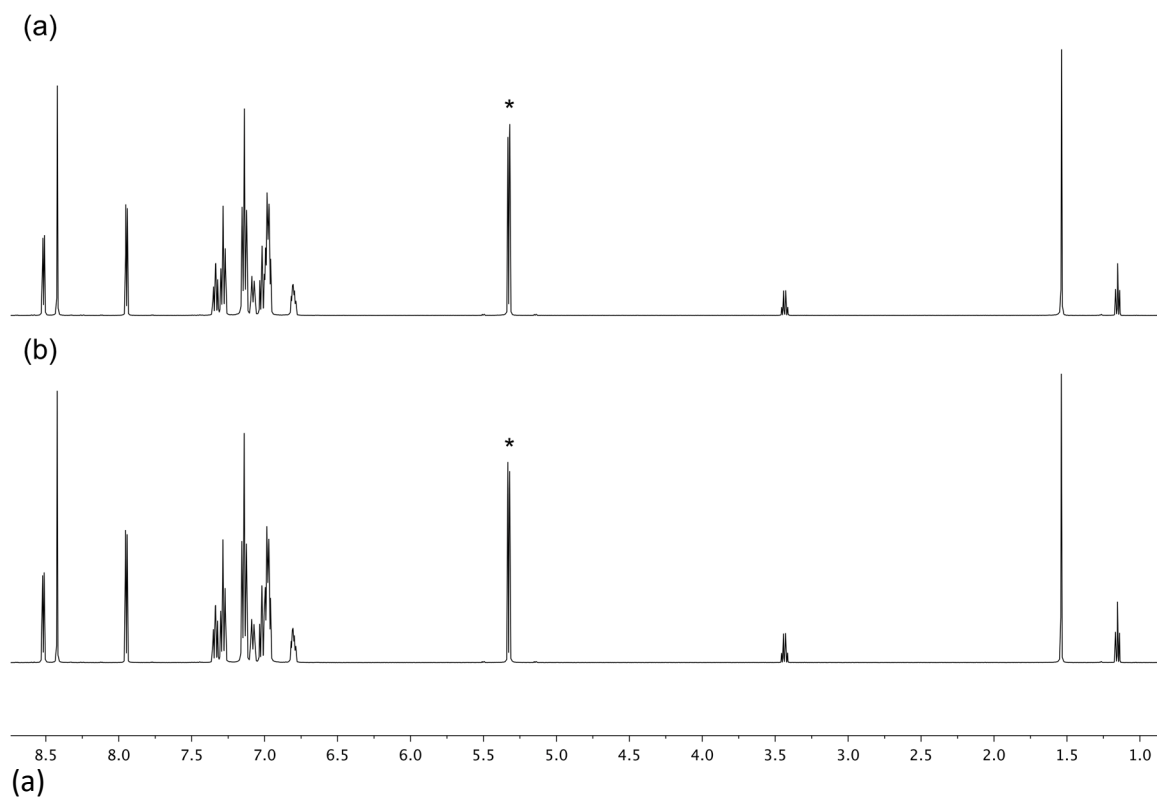


Fig. S25. HMBC spectrum (aromatic region, 500 MHz ^1H , 126 MHz $^{13}\text{C}\{^1\text{H}\}$, acetone- d_6 , 298 K) of $[\text{Cu}(\text{xantphos})(4,7\text{-Br}_2\text{phen})][\text{PF}_6]$.



(b)

Fig. S26. (a) ^1H NMR spectrum (500 MHz, CD_2Cl_2 , 298 K, aromatic region) of $[\text{Cu}(\text{POP})(4,7\text{-Br}_2\text{phen})][\text{PF}_6]$: (a) after freshly preparing the NMR sample and (b) after 6 hours standing at room temperature. (b) NOESY spectrum (500 MHz, CD_2Cl_2 , 298 K, aromatic region) of $[\text{Cu}(\text{POP})(4,7\text{-Br}_2\text{phen})][\text{PF}_6]$.

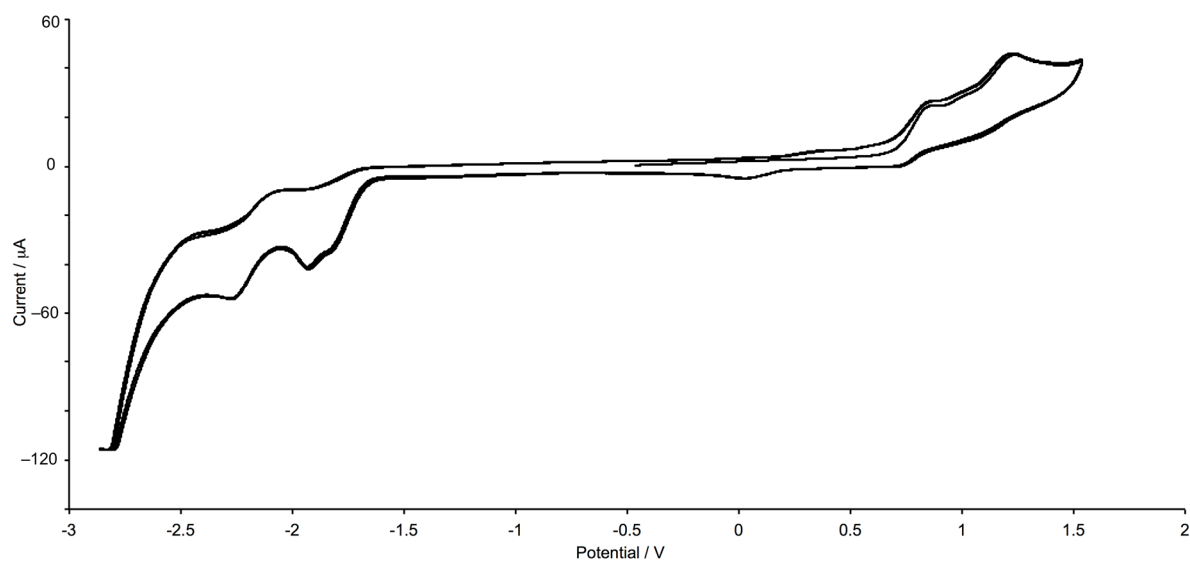
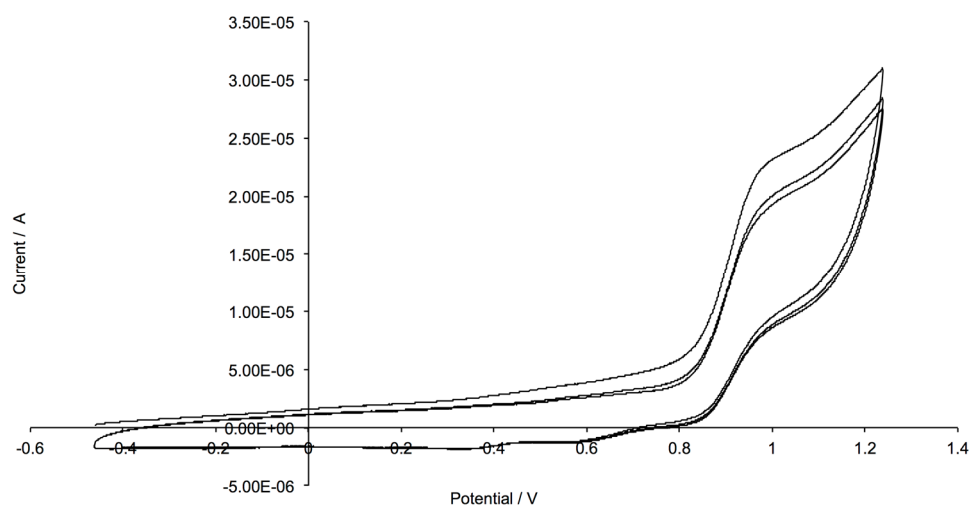
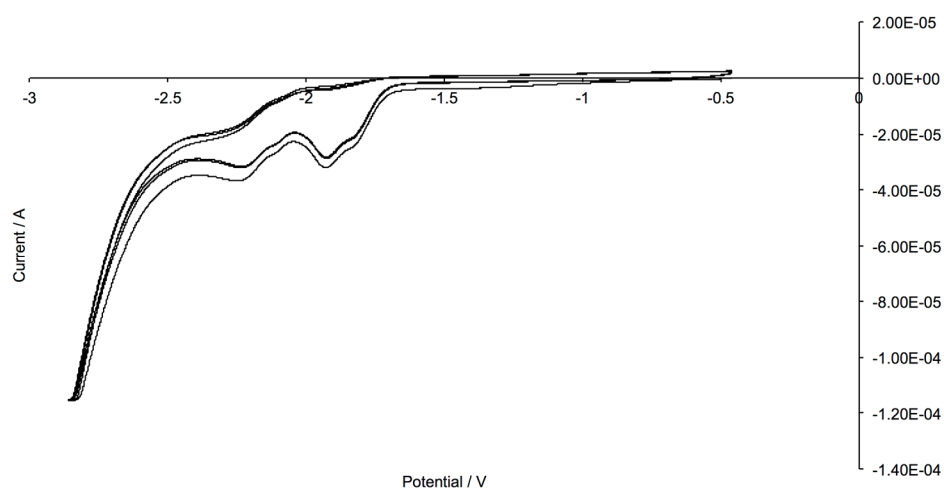


Fig. S27. Representative CV showing two successive cycles for $[\text{Cu}(\text{POP})(4,7\text{-Br}_2\text{phen})][\text{PF}_6]$. Referenced to internal $\text{Fc}/\text{Fc}^+ = 0.0 \text{ V}$; CH_2Cl_2 solution with $[\text{nBu}_4\text{N}][\text{PF}_6]$ as supporting electrolyte and scan rate of 0.1 V s^{-1} .

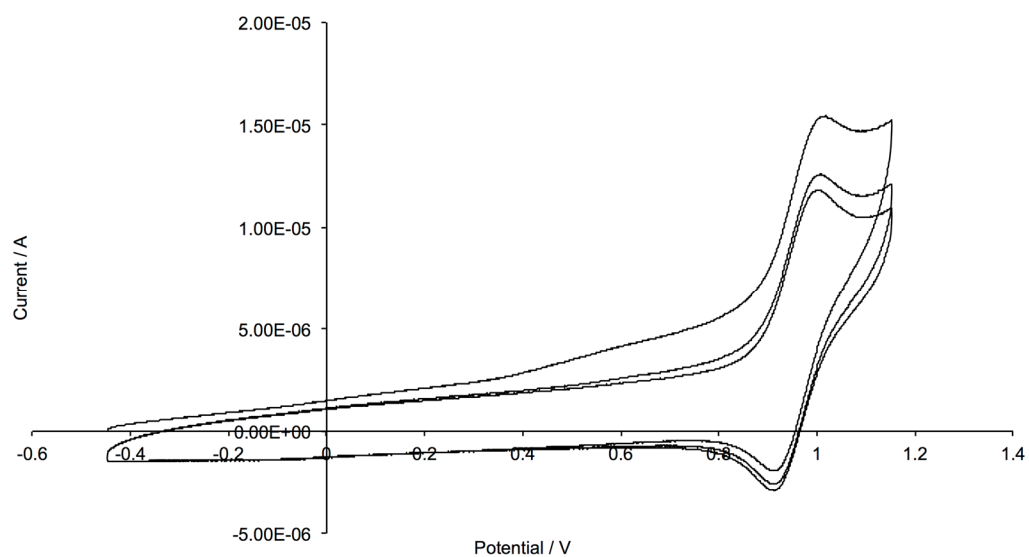


(a)

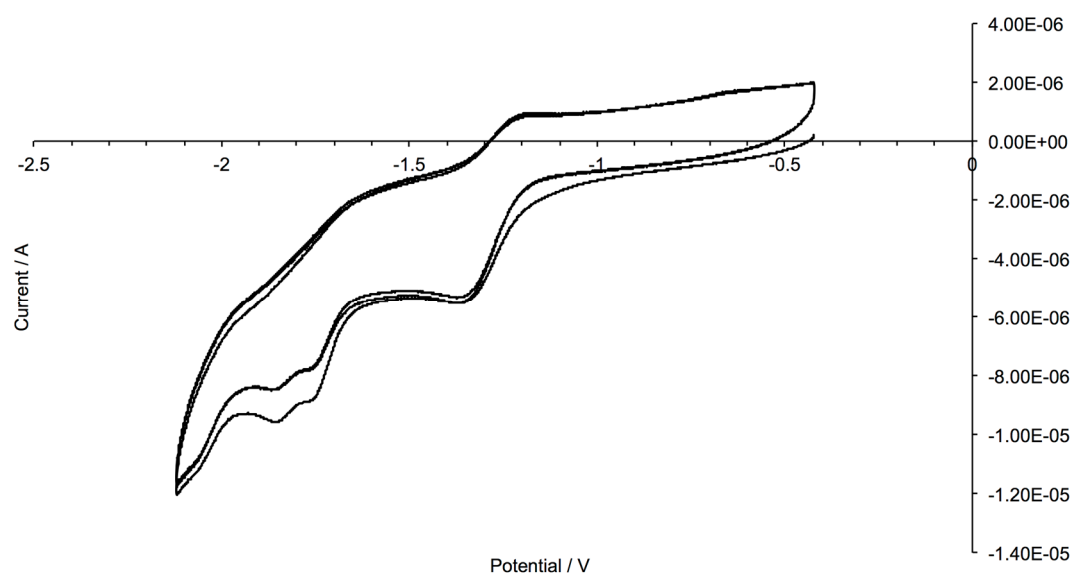


(b)

Fig. S28. Successive cycles in the (a) anodic and (b) cathodic scans for $[\text{Cu}(\text{POP})(2,9\text{-Br}_2\text{phen})][\text{PF}_6]$. Referenced to internal $\text{Fc}/\text{Fc}^+ = 0.0 \text{ V}$; CH_2Cl_2 solution with $[\text{nBu}_4\text{N}][\text{PF}_6]$ as supporting electrolyte and scan rate of 0.1 V s^{-1} .



(a)



(b)

Fig. S29. Successive cycles in the (a) anodic and (b) cathodic scans for $[\text{Cu}(\text{xantphos})(2,9\text{-Br}_2\text{phen})][\text{PF}_6]$. Referenced to internal $\text{Fc}/\text{Fc}^+ = 0.0 \text{ V}$; CH_2Cl_2 solution with $[\text{tBu}_4\text{N}][\text{PF}_6]$ as supporting electrolyte and scan rate of 0.1 V s^{-1} .

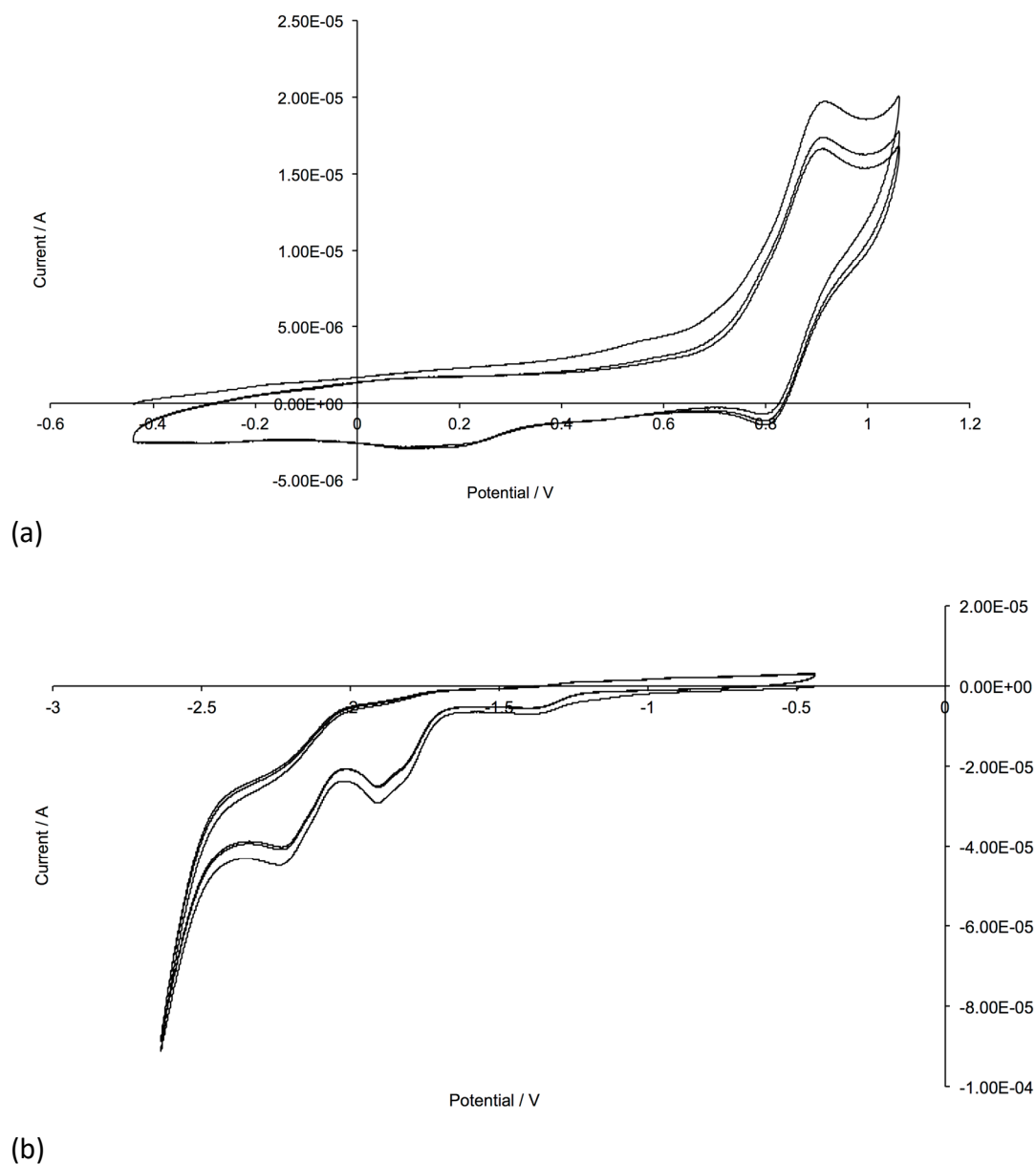


Fig. S30. Successive cycles in the (a) anodic and (b) cathodic scans for $[\text{Cu}(\text{POP})(3,8\text{-Br}_2\text{phen})][\text{PF}_6]$. Referenced to internal $\text{Fc}/\text{Fc}^+ = 0.0 \text{ V}$; CH_2Cl_2 solution with $[\text{nBu}_4\text{N}][\text{PF}_6]$ as supporting electrolyte and scan rate of 0.1 V s^{-1} .

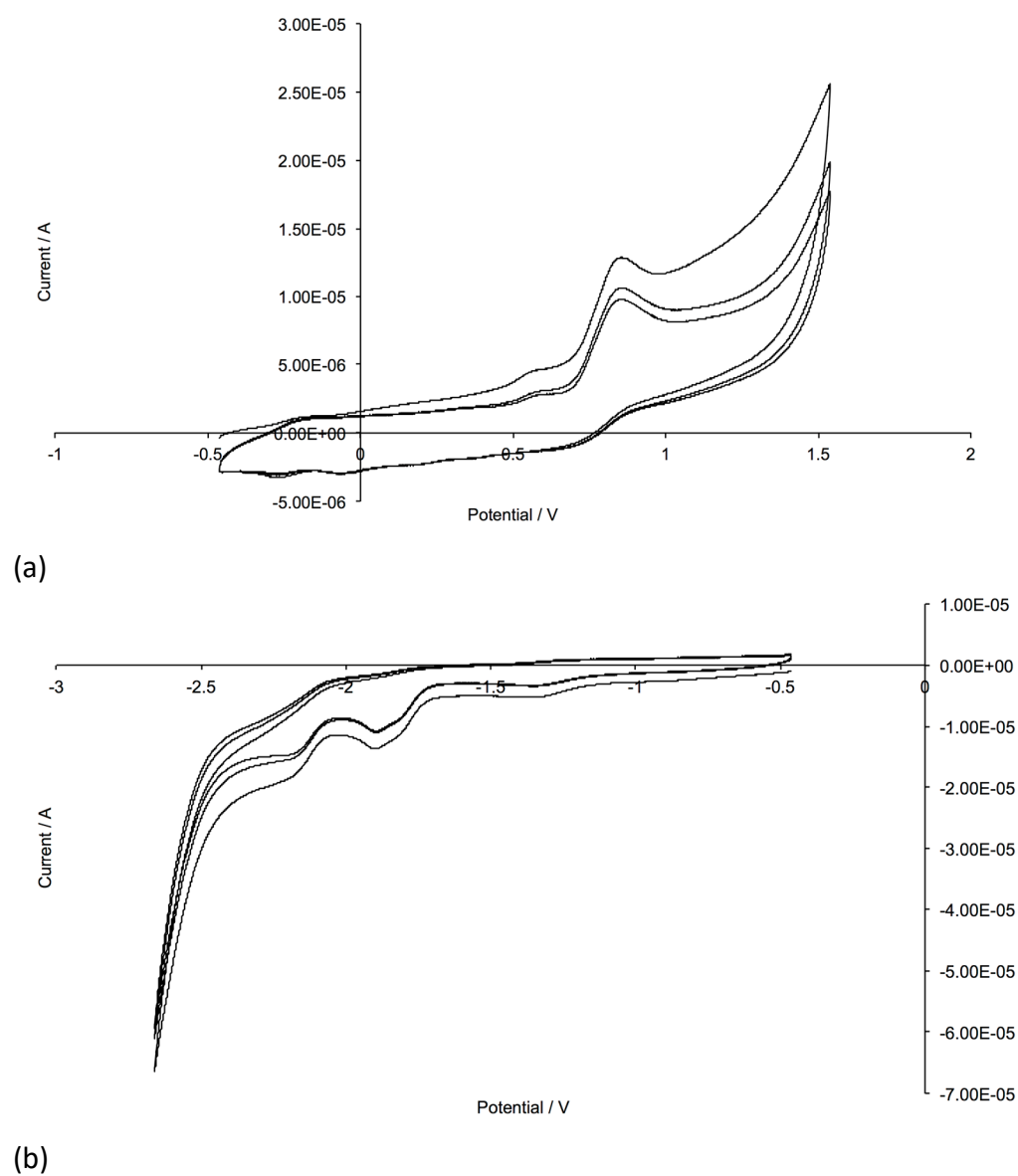


Fig. S31. Successive cycles in the (a) anodic and (b) cathodic scans for $[\text{Cu}(\text{xantphos})(3,8\text{-Br}_2\text{phen})][\text{PF}_6]$. Referenced to internal $\text{Fc}/\text{Fc}^+ = 0.0 \text{ V}$; CH_2Cl_2 solution with $[\text{nBu}_4\text{N}][\text{PF}_6]$ as supporting electrolyte and scan rate of 0.1 V s^{-1} .

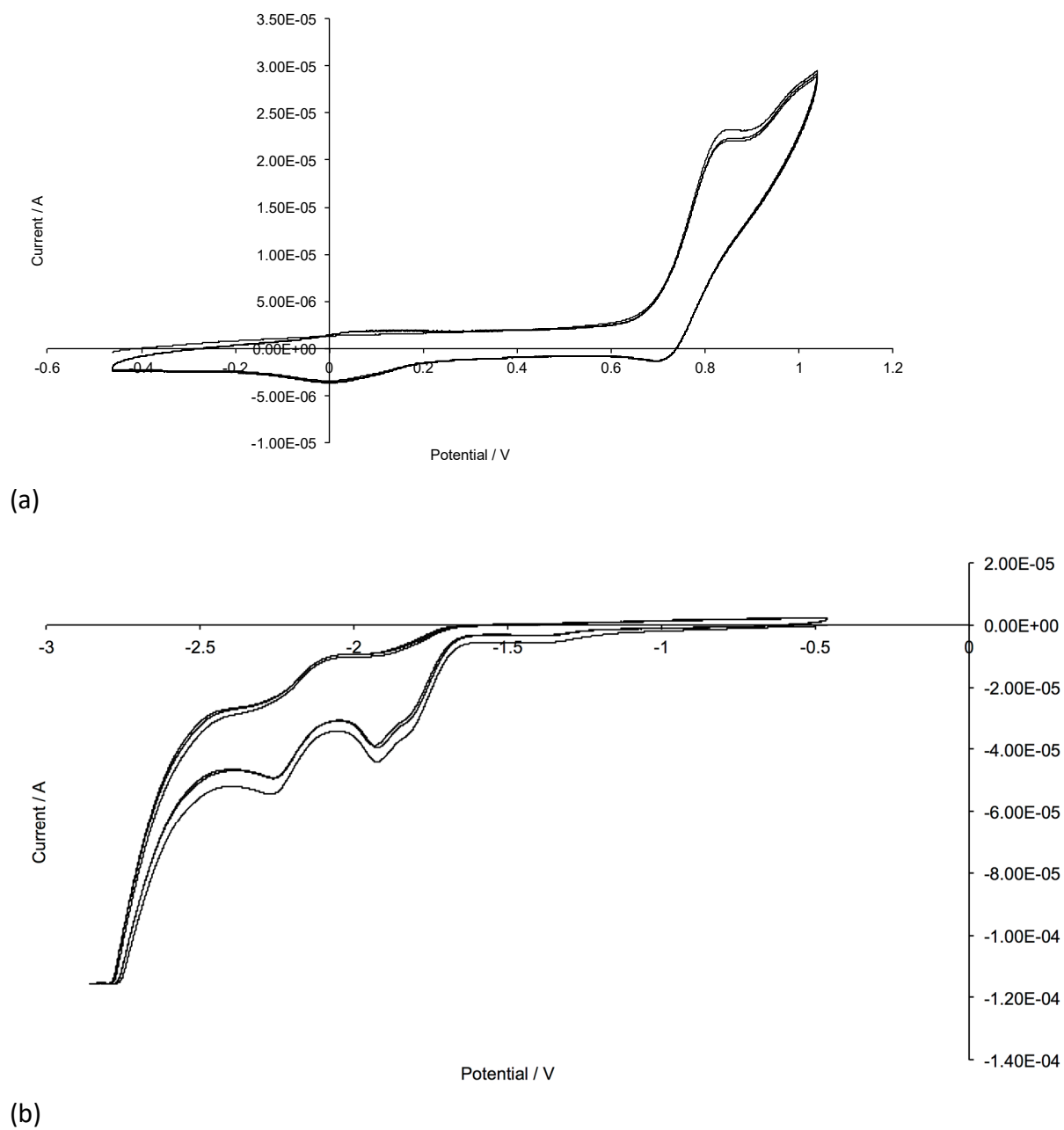


Fig. S32. Successive cycles in the (a) anodic and (b) cathodic scans for $[\text{Cu}(\text{POP})(4,7\text{-Br}_2\text{phen})][\text{PF}_6]$. Referenced to internal $\text{Fc}/\text{Fc}^+ = 0.0 \text{ V}$; CH_2Cl_2 solution with $[\text{nBu}_4\text{N}][\text{PF}_6]$ as supporting electrolyte and scan rate of 0.1 V s^{-1} .

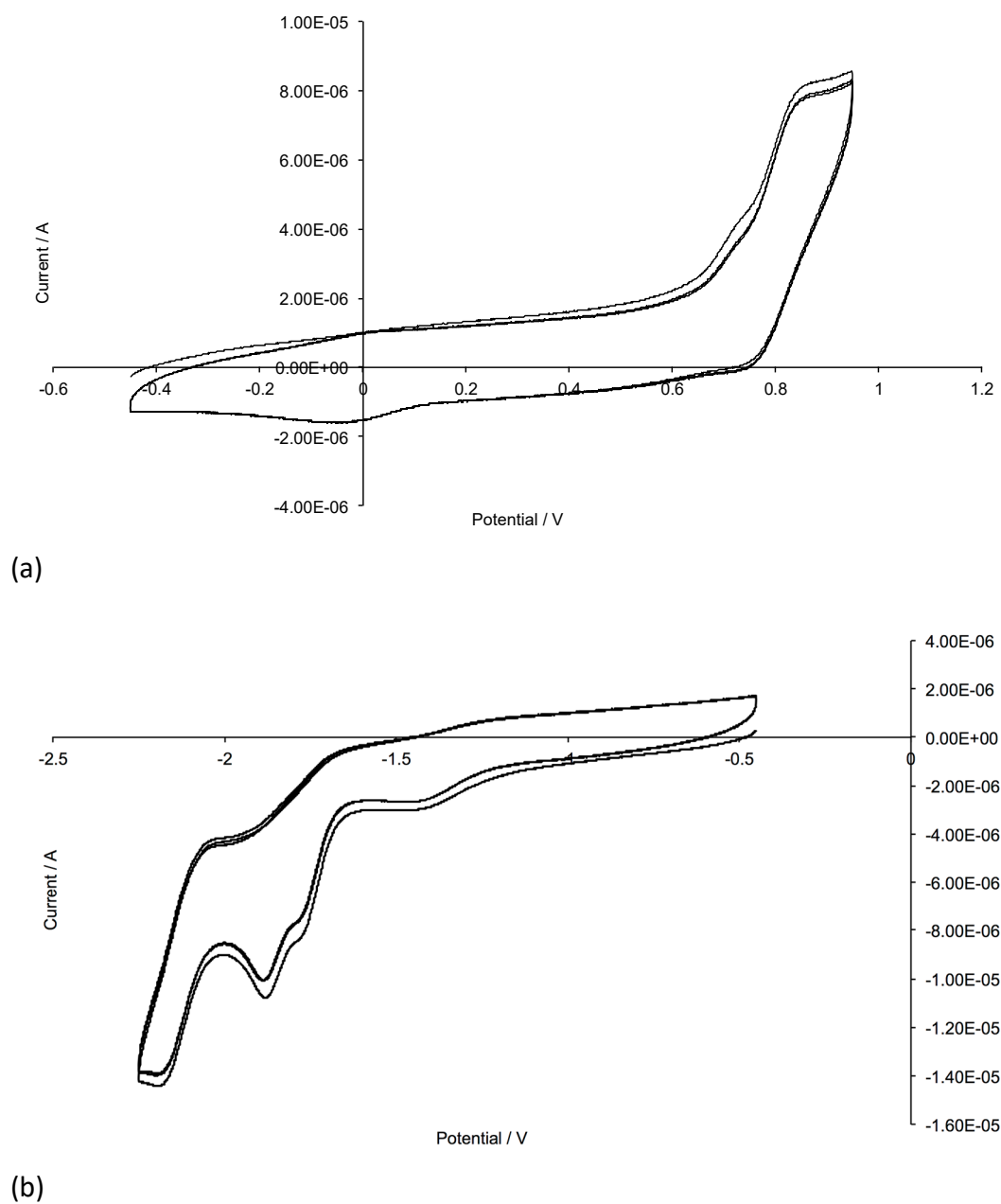


Fig. S33. Successive cycles in the (a) anodic and (b) cathodic scans for $[\text{Cu}(\text{xantphos})(4,7\text{-Br}_2\text{phen})][\text{PF}_6]$. Referenced to internal $\text{Fc}/\text{Fc}^+ = 0.0 \text{ V}$; CH_2Cl_2 solution with $[\text{nBu}_4\text{N}][\text{PF}_6]$ as supporting electrolyte and scan rate of 0.1 V s^{-1} .